

Direct observation of superconducting vortex clusters pinned by a periodic array of magnetic dots in ferromagnetic/superconducting hybrid structures.

T. Shapoval*,¹ V. Metlushko,² M. Wolf,¹ B. Holzapfel,¹ V. Neu,¹ and L. Schultz¹

¹IFW Dresden, Institute for Metallic Materials, P.O. Box 270116, D-01171 Dresden, Germany.

²Department of Electrical and Computer Engineering,
University of Illinois at Chicago, Illinois 60612, USA.

Strong pinning of superconducting flux quanta by a square array of $1\ \mu\text{m}$ -sized ferromagnetic dots in a magnetic-vortex state was visualized by low-temperature magnetic force microscopy (LT-MFM). A direct correlation of the superconducting flux lines with the positions of the dots was derived. The force that the MFM tip exerts on the individual vortex in the depinning process was used to estimate the spatial modulation of the pinning potential. It was found, that the superconducting vortices which are preferably located on top of the Py dots experience about 15 times stronger pinning forces as compared to the pinning force in the pure Nb film. The strong pinning exceeds the repulsive interaction between the superconducting vortices and allows the vortex clusters to be located at each dot. Our microscopic studies are consistent with global magnetoresistance measurements on these hybrid structures.

PACS numbers: 74.70.-b 74.78.-w 74.25.Qt 68.37.Rt

Controlling the distribution of magnetic flux quanta (superconducting vortices) in superconducting materials by introducing artificial pinning centers is a challenge, both in basic and in applied research. Due to the presence of the natural point disorder (e.g. grain and intergrain pinning) in superconducting thin films superconducting vortices form a weakly disordered Abrikosov lattice [1], so called topologically ordered Bragg glass [2]. In the last decade a variety of studies has been performed to investigate the influence of different artificial pinning centers on the superconducting properties of thin films [3, 4, 5, 6, 7]. On the one hand, randomly distributed defects act as strong local pinning centers which significantly improve the in-field critical parameters of superconducting films [4], on the other hand, ordered pinning potentials give rise to collective pinning mechanisms and thus lead to commensurate pinning effects [3, 5, 8]. In comparison to simple structurally ordered pinning sites, magnetic pinning centers provide additional degrees of freedom, which lead to several pronounced effects, such as domain-wall superconductivity, field induced superconductivity, proximity effect, magnetostatic interaction, and local suppression of superconductivity by strong out-of-plane field components [6, 7], some of which can be used to tune vortex dynamics by rectifying vortex motion [9].

In this work, the interplay between superconducting and magnetic vortices in ferromagnetic/superconducting (FM/SC) hybrid structures with well-controlled lateral dimension is visualized by low-temperature magnetic force microscopy (LT-MFM) using a commercial scanning probe microscope (*Omicron Cryogenic SPM*) [10]. The MFM cantilever (Nanoworld MFMR) possesses a force constant of about $2.8\ \text{N/m}$ and a resonance frequency of about $80\ \text{kHz}$. The measured shift of the cantilever's resonance frequency Δf is proportional to the derivative of the z component of the force that acts between the tip and the sample at a given scanning distance above the surface [11].

The following hybrid structure is studied: a square array of permalloy (Py = $\text{Ni}_{80}\text{Fe}_{20}$) dots with $1\ \mu\text{m}$ diame-

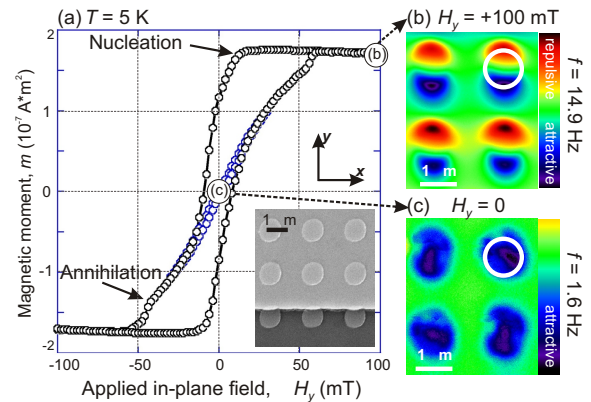


Fig. 1: (a) Magnetic hysteresis loop shows magnetic vortex behavior with vortex nucleation and annihilation fields. Within the inner loop, between $-30\ \text{mT}$ and $+30\ \text{mT}$, the magnetization is reversible. The inset shows a SEM image of Py dots covered with a $100\ \text{nm}$ thick Nb layer. The in-plane field H_y was varied along the hysteresis loop starting from saturation at $+100\ \text{mT}$ (b), through applying a negative field less than the magnetic-vortex annihilation field ($-25\ \text{mT}$) to the magnetic-vortex state at zero field (c). Color bars give the measured Δf signal which strongly differs between the saturated and the vortex state. A small out-of-plane field of $+10\ \text{mT}$ was permanently applied to insure a positive polarity of the magnetic vortex. Scanning distance was $75\ \text{nm}$, $T = 14.6\ \text{K}$. The white circles represent the location of the Py dot.

ter, $25\ \text{nm}$ height and $2\ \mu\text{m}$ periodicity was prepared on a Si (100) substrate using standard e-beam lithography, e-beam evaporation, and lift-off processes; a $100\ \text{nm}$ thick superconducting niobium (Nb) ($T_c = 8.32\ \text{K}$) was deposited on top of the Py dot array by sputter deposition [12]. A SEM scan of this Py/Nb hybrid structure is shown in Fig. 1 (a) (inset).

Depending on their shape and aspect ratio, ferromagnetic dots can be in different magnetization states such as multidomain, single domain or, for the circular dots, a magnetic-vortex state becomes energetically stable at remanence [13]. Here, the magnetization curls continuously around the cen-

ter while staying purely in-plane in a large area of the dot and turns perpendicular to the surface in the center of the dot creating a small magnetization swirl [14, 15]. This swirl, also called a magnetic-vortex core, has either positive or negative polarity of its out-of-plane stray field and has a maximum width of $5l_{\text{ex}} \approx 25$ nm for the present geometry, with $l_{\text{ex}} = \sqrt{A/K_d}$ being the exchange length, where A is the material specific exchange stiffness constant and K_d is the stray field energy constant [15].

Hoffmann *et al.* have reported a clear correlation between a strong drop in the resistivity curve for a SC Nb film and the magnetic-vortex state of the underlying Py dots, which was shown to be independent of the polarity of the magnetic-vortex core [12]. In the present work, local imaging was applied to look deeper into the nature of this enhanced pinning, providing a direct determination of the preferable locations of SC vortices, as well as an estimation of the local pinning force by observing the depinning of individual SC flux lines.

The magnetic in-plane hysteresis loop [Fig. 1 (a)] of the Py array measured at 5 K using a superconducting quantum interference device (SQUID) clearly reveals magnetic vortex behavior with vortex nucleation and annihilation fields. For the inner loop in the field range from -30 mT to $+30$ mT, the magnetization process occurs only by vortex propagation and, thus, is reversible (vortex branch).

To reach the magnetic-vortex configuration in the Py array, the sample was cooled in the microscope down to 40 K. An in-plane field of $+100$ mT was applied along the positive y direction (H_y) to fully saturate the dots, and the sample was further cooled down to 14.6 K. The MFM scan at a tip-sample distance of 75 nm shows four saturated Py dots [Fig. 1 (b)]. Decreasing the field to -25 mT ensures that in most of the dots a magnetic vortex is nucleated. Going back to zero along the vortex branch brings the dots into the symmetric magnetic-vortex state imaged in Fig. 1 (c). Magnetic vortices, generated in such a way, will have random polarity (i.e. out-of-plane magnetization components pointing randomly up or down) [16]. To set a defined polarity, a small positive out-of-plane field ($+10$ mT) was applied to the sample during the above-described field sequence. Thus, the magnetic-vortex core and the MFM tip, which is magnetized in positive z -direction, experience an attractive interaction that shows up as a dark contrast in the center of the dot [Fig. 1 (c)].

After reaching the magnetic-vortex state of the Py dots the sample was repeatedly cooled down to a temperature below T_c of the Nb film ($T = 6.1$ K $\approx 72\%$ T_c) in perpendicular fields $H_{\text{applied}} = +0.5$ mT, 0, -0.5 mT and -1 mT that are close to the matching fields for this hybrid structure. The matching field H_m is a field that ensures an integer number m of vortices per unit area S of the dot array: $H_m = m\Phi_0/S$, with $\Phi_0 = h/2e$ being the magnetic flux quantum [3].

An area where one dot is not fully switched to the magnetic-vortex state and has a residual in-plane component was chosen for LT-MFM imaging to confirm that the same dots are imaged at different fields and to correct a

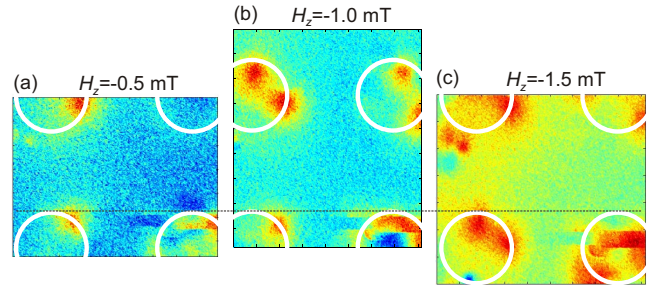


Fig. 2: Visualization of superconducting vortices pinned by Py dots at 6.1 K ($72\%T_c$). For a better visualization of the vortex positions the “background” image was subtracted. The frozen effective fields ΔH_z are: (a) -0.5 mT, (b) -1 mT and (c) -1.5 mT. SC vortices are visualized as red spots.

small thermal drift. It was established that the vertical coil of the microscope has a shift of zero point in the range of -0.5 mT. This justifies to consider the $+0.5$ mT image, where only magnetic contrast from the Py dots is observed, as a “background”, and to subtract it from the other ones. The results are shown in Fig. 2 (a)–(c), respectively, and correspond to the effective fields $\Delta H_z = H_{\text{applied}} - 0.5$ mT. The orientation of ΔH_z is negative, so that SC vortices and the MFM tip exhibit repulsive interaction (red color). Hence, the SC vortices in Nb film have a polarity opposite to that of the magnetic-vortex core in Py dots. This means that the magnetostatic interaction between magnetic and SC vortices is repulsive. Such a configuration is selected to differentiate the magnetostatic pinning mechanism from the non-magnetic one.

Fig. 2 (a) corresponds to the first matching field H_1 . Here one SC vortex, as expected, is visualized per unit area of the dot array. The SC vortices are located on top of the Py dots (white circles), showing that the dots work as preferable pinning centers. Nevertheless, they do not concentrate at the center of the dot, but occupy the edges of the dot. Furthermore, no SC vortices are visualized in the interstitial positions. This effect becomes more pronounced in Fig. 2 (b) where the second matching field H_2 has been applied during cooling. Also here, despite the long-range repulsive interaction between SC vortices, they are not distributed homogeneously, but are strongly pinned by the Py dots, so that two vortices are located on each dot. A further increase of the field to H_3 leads to an enhanced magnetic contrast on top of the Py dots, which corresponds to multiple flux quanta (vortex cluster) pinned by the dots [Fig. 2 (c)]. Here the expected three SC vortices could not be separately resolved due to overlapping of their magnetic stray fields at small vortex-vortex distances. The dark blue contrast that appears on one magnetic dot in this field (lower left dot) can be explained by the shift of the magnetic-vortex core and changing of the magnetization state of the dot by the stray field coming out of the agglomeration of three SC vortices. This dark blue contrast is stable and exists even at temperatures slightly above T_c of the Nb film (image not shown here).

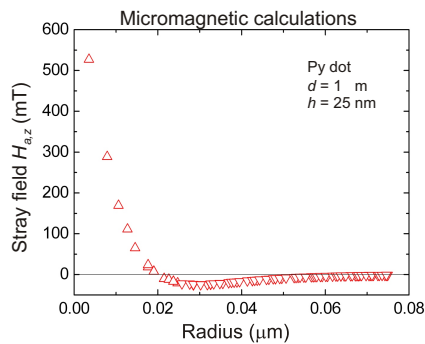


Fig. 4: Stray field distribution just above the surface of the Py dot in the vortex state. The estimated values are based on micromagnetic calculations using the LLG-program [19].

larity should be located directly at the magnetic vortex core. Another mechanism is based on the local suppression of superconductivity due to the highly localized out-of-plane field produced by the magnetic-vortex core (core pinning) [12]. Here, the magnetostatic interaction is negligible, and the SC vortices are located at the magnetic-vortex core independent of their polarity. Nevertheless, neither of these mechanisms can fully explain the situation reported in the present work.

To exclude the possibility that the SC vortices are magnetostatically attracted by the returning stray field lines of the magnetic vortex, the stray field distribution just above the surface of a Py dot in the magnetic-vortex state was estimated by micromagnetic calculations [19]. The estimated stray field for the Py dot geometry used in the above-described experiments reveals that such negative field values are found already close to the distances of 25 nm from the center of the dot (Fig. 4). Hence, the simple attractive magnetostatic interaction between the SC vortex and the returning stray field of the magnetic vortex could not provoke the visualized arrangement of the SC vortices being located almost at the edges of the Py dot [Fig. 2 (b)].

In summary, we have demonstrated microscopically that the presence of magnetic vortices underneath the superconducting Nb film significantly influences the natural pinning landscape. The superconducting vortices are preferably located on top of the Py dots, undergoing an about 15 times stronger pinning force at the Py dots compared to the pure Nb film. This pinning force overcomes the repulsive interaction between the SC vortices, allowing the SC vortex clusters be to pinned by each dot. Our local magnetic force microscopic studies of the superconducting vortex distribution in the presence of an array of ferromagnetic dots with well controlled lateral dimensions are consistent with the global magnetoresistance measurements. Nevertheless, the reported local arrangement of the superconducting vortices

could not be fully interpreted by the existing scenarios.

Acknowledgements. The work was partially funded by the European Community under the 6th Framework Programme Contract Number 516858: HIPERCHEM and by the U.S. NSF grant ECCS-0823813. Image processing was done using the WSxM 4.0 software [20]. The authors thank the ESF for financing a conference visit that resulted in a fruitful cooperation. The authors acknowledge discussions with E. Backen and S. Haindl, thank D.S. Inosov and R. Schäfer for critical reading of the manuscript and U. Wolff for the MFM tip preparation.

*Corresponding author: t.shapoval@ifw-dresden.de

- [1] A. A. Abrikosov, *Sov. Phys. JEPT* **5**, 1174 (1957).
- [2] T. Giamarchi *et al.*, *Phys. Rev. B* **55**, 6577 (1997).
- [3] V. V. Moshchalkov *et al.*, *Phys. Rev. B* **54**, 7385 (1996).
- [4] S. R. Foltyn *et al.*, *Nature Materials* **6**, 631 (2007).
- [5] A. Bezryadin *et al.*, *Phys. Rev. B* **53**, 8553 (1996); V. Metlushko *et al.*, *ibid.* **59**, 603 (1999); V. V. Moshchalkov *et al.*, *ibid.* **57**, 3615 (1998); C. Reichhardt *et al.*, *ibid.* **57**, 7937 (1998); *Phys. Rev. Lett.* **78**, 2648 (1997); S. B. Field *et al.*, *ibid.* **88**, 067003 (2002); M. Baert *et al.*, *ibid.* **74**, 3269 (1995); Z. Jiang *et al.*, *Appl. Phys. Lett.* **84**, 5371 (2004); A. A. Zhukov *et al.*, *ibid.* **83**, 4217 (2003).
- [6] A. Yu. Aladyshkin *et al.*, *Supercond. Sci. Technol.* **22**, 053001 (2009).
- [7] J. I. Martin *et al.*, *Phys. Rev. Lett.* **79**, 1929 (1997); D. J. Morgan *et al.*, *ibid.* **80**, 3614 (1998); M. J. Van Bael *et al.*, *ibid.* **86**, 155 (2001); J. E. Villegas *et al.*, *ibid.* **99**, 227001 (2007); *Science* **302**, 1188 (2003); Y. Jaccard *et al.*, *Phys. Rev. B* **58**, 8232 (1998); S. Erdin *et al.*, *ibid.* **66**, 014414 (2002); M. J. Van Bael *et al.*, *ibid.* **68**, 014509 (2003); A. V. Silhanek *et al.*, *Appl. Phys. Lett.* **89**, 182505 (2006); *ibid.* **90**, 182501 (2007); S. Haindl *et al.*, *Supercond. Sci. Technol.* **21**, 045017 (2008).
- [8] U. Patel *et al.*, *Phys. Rev. B* **76**, 020508(R) (2007).
- [9] C. C. de Souza Silva *et al.*, *Phys. Rev. Lett.* **98**, 117005 (2007); G. Carneiro, *Physica C* **432**, 206 (2005).
- [10] T. Shapoval *et al.*, *Physica C* **460-462**, 732 (2007).
- [11] T. R. Albrecht *et al.*, *J. Appl. Phys.* **69**, 668 (1991).
- [12] A. Hoffmann *et al.*, *Phys. Rev. B* **77**, 060506(R) (2008).
- [13] M. Schneider *et al.*, *Appl. Phys. Lett.* **77**, 2909 (2000); T. Shinjo *et al.*, *Science* **289**, 930 (2000).
- [14] A. Wachowiak *et al.*, *Science* **298**, 577 (2002).
- [15] A. Hubert and R. Schäfer, *Magnetic Domains*, Springer Berlin (2009).
- [16] J. E. Villegas *et al.*, *Phys. Rev. B* **77**, 134510 (2008).
- [17] J. Pearl, *Appl. Phys. Lett.* **5**, 65 (1964).
- [18] E. W. J. Straver *et al.*, *Appl. Phys. Lett.* **93**, 172514 (2008); O. M. Auslaender *et al.*, *Nature Physics* **5**, 35 (2009).
- [19] M. R. Scheinfein, *The LLG Micromagnetics Simulator*TM <http://llgmicro.home.mindspring.com>.
- [20] I. Horcas *et al.*, *Rev. Sci. Instrum.* **78**, 013705 (2007).